

# Macrostructural characterization of granular activated carbon beds

M. C. MAUGUET, A. MONTILLET\*, J. COMITI\*

GEPEA, Laboratoire de Génie des Procédés Environnement Agroalimentaire,  
UMR-CNRS 6144, CRTT, bd de l'Université, BP 406, 44602 Saint-Nazaire Cedex, France  
E-mail: agnes.montillet@univ-nantes.fr  
E-mail: jacques.comiti@univ-nantes.fr

Scale-up and prediction of performance of granular activated carbon (GAC) fixed bed adsorbers require the knowledge of the structural parameters of the particles and of the corresponding beds. A set of suitable and relatively simple methods including alumina and helium pycnometry, image analysis and water permeametry are therefore proposed and validated in this paper. These methods allow determination of particle parameters like internal porosity, particle density, solid density and size distribution. The bed characteristics obtained by applying the proposed approach are bed porosity, bed dynamic specific surface area and tortuosity. Experimental results obtained with this approach and concerning two kinds of GAC particle shape are given in this paper. © 2005 Springer Science + Business Media, Inc.

## Nomenclature

$a_v$	Specific surface area obtained by BET measurement ( $m^{-1}$ )
$a_{vd}$	Dynamic specific surface area of porous medium ( $m^{-1}$ )
$a_{vs}$	Static specific surface area of porous medium ( $m^{-1}$ )
$d_{pore}$	Diameter of the pores defined in the capillary model (m) (Equation 5)
$d_p$	Particle diameter (m)
$d_{pe}$	Equivalent mean diameter of particle (m)
$D$	Column diameter (m)
$D_m$	Average diameter of the NC 60 particle size distribution (m)
$D_{mould}$	Diameter of mould (m)
GAC	Granular activated carbon
$H$	Height of fixed bed (m)
$H_c$	Height of the column (m)
$L$	Length of the pores defined in the capillary model (m)
$L_m$	Average length of the extruded particle size distribution (m)
$L_{mould}$	Length of the mould (m)
$m$	Mass of material sample (kg)
$Re_{pore}$	Pore Reynolds number (Equation 7)
$U$	Mean velocity in the pore ( $m \cdot s^{-1}$ ) (Equation 6)
$U_0$	Superficial velocity of the fluid in the packed bed ( $m \cdot s^{-1}$ )
$V_{bed}$	Bed volume in cylindrical column ( $m^3$ )
$V_{pore}$	Internal pore volume developed in the particles ( $m^3$ )

$V_s$	Volume of solid phase ( $m^3$ )
$V_{sample}$	Global volume developed by the particles in the sample ( $m^3$ )

## Greek letters

$\delta$	Mean relative error (Equation 10)
$\varepsilon_i$	Internal porosity (particle porosity)
$\varepsilon_{ext}$	External porosity
$\eta$	Dynamic viscosity (Pa s)
$\nu$	Kinematic viscosity ( $m^2 \cdot s^{-1}$ )
$\rho_b$	Bulk or bed density ( $kg \cdot m^{-3}$ )
$\rho_0$	Fluid density ( $kg \cdot m^{-3}$ )
$\rho_p$	Particle density ( $kg \cdot m^{-3}$ )
$\rho_s$	Solid density ( $kg \cdot m^{-3}$ )
$\tau$	Tortuosity (Equation 4)

## 1. Introduction

Activated carbons, due to their well-known adsorbent properties are widely used in different industrial domains, especially for the removal of dissolved organic pollutants from water and wastewater by means of fixed bed columns made of granular activated carbon (GAC) [1]. The efficiency of such adsorbers is directly linked to the molecule adsorption kinetic presented by the GAC bed [2–4]. Such kinetics are very complex and depend on fluid flow, mass transfer (internal and external to the particles), and on physical and chemical structures presented by the bed as well as the GAC particles. In order to reach a better understanding of these kinetics and therefore to improve the depollution performance of this treatment method, many works

\*Authors to whom all correspondence should be addressed.

in the literature have so far investigated the physical and chemical characterization of the GAC particles. To this aim, more and more accurate methods (adsorption method, thermogravimetry, colorimetry, probe molecule retention. . .) are used to determine the influence of different microstructural parameters on adsorption such as internal porosity, pore size distribution, specific surface area, nature and quantity of surface groups [5–8].

The prediction of the performance of adsorption devices also requires the determination of macrostructural parameters such as external porosity, particle density, specific surface area, and tortuosity. Although the determination of non porous fixed-bed structural parameters is not a new research subject, in the case of microporous porous media like GAC bed, the technical application of these methods and especially the evaluation of external porosity proved to be limited or impossible to use owing to the complexity of the microporous network.

The aim of this work is then to assess different macrostructural parameters of two commercially available GAC by proposing a set of operating modes checked out for this type of material and validated independently. The choice of the methods was based on two criteria: simplicity of implementation and accuracy of the results.

The next section describes the main parameters, which characterize the macrostructure as well as the possible means of obtaining them. A discussion and a presentation of the adopted experimental procedure close this part. Experimental details and results are given in a following section.

## 2. Structural and particle parameters

### 2.1. Particle size distribution

The knowledge of the particle size distribution is important due to its effect on the bed structure and consequently on the external bed porosity value. The granulometric analysis consists in the classification of the set of particles (so-called representative sample of a batch studied) according to a given size criterion. For each class a frequency is associated, defined usually as the ratio between the number of particles of the size-interval considered and the total number of particles constituting the representative sample.

The granulometric analysis methods are numerous: sieving, sedimentation, laser granulometry and image analysis are the most commonly employed methods to elaborate an histogram of size repartition [9]. Table I recaps the principle of these various methods as well as their advantages and drawbacks [10].

### 2.2. Density of activated carbon particles

The determination of parameters such as density and pore volume is necessary to evaluate the bed porosity (internal and external porosity in our case). Under the generic term of density, different notions are regrouped. Thus, in the reference book of Lowell and Shields [11], six different densities are indexed. In our work, three

of these densities are relevant: bulk, particle and solid densities, respectively represented by  $\rho_b$ ,  $\rho_p$ ,  $\rho_s$ .

#### 2.2.1. Solid density

This density,  $\rho_s$ , represents the ratio between the mass,  $m$ , of the material and the corresponding volume  $V_s$ , occupied by the material solid phase. If a powder presents no internal porosity, the solid density can be measured by displacement of any liquid in which the solid remains inert. However, the solid usually contains pores, cracks, or crevices, which are incompletely penetrated by a displaced liquid. In this case,  $\rho_s$  can be measured by using as the displaced fluid a gas. Helium is the most frequently used gas because the inertness and small size of the helium atom enables it to penetrate even the smallest pores. Mercury porosimeter can also be a convenient method for measuring the density of powders in some particular cases. Indeed, it gives the true density of powders without pores or without voids smaller than those into which intrusion occurs at the highest pressure attainable in the porosimeter. This technique also allows to get the apparent density in the case of powders that have only pores smaller than those corresponding to the highest pressure allowed by the apparatus.

#### 2.2.2. Bulk density

The bed or bulk density,  $\rho_b$ , is the mass of adsorbent in a specific volume. This can simply be measured using a graduated cylindrical column.

#### 2.2.3. Particle density

The particle density,  $\rho_p$ , is the mass of adsorbent per volume occupied by the particle (solid and internal pore volume).

## 2.3. External and internal porosities of activated carbons beds

### 2.3.1. External porosity

The external porosity,  $\varepsilon_{\text{ext}}$ , of activated carbon beds corresponds to the ratio of the volume of interparticle spaces to the total bed volume. Commonly, if the particle density is known, it is evaluated by a direct calculation using this expression,

$$\varepsilon_{\text{ext}} = 1 - \frac{\left(\frac{m}{\rho_p}\right)}{V_{\text{bed}}} \quad (1)$$

In the literature, few works dealt with the characterization of the macrostructure of porous beds, by attempting to correlate the porosity of the bed to different characteristic parameters (as for example the particles shape, the ratio between particle diameter and column diameter. . .) [12–15]. In most cases, the particles studied are solid spheres or cylinders without microporosity. This parameter can be very easily evaluated in the case of non porous materials. On the opposite its determination is not direct in the case of microporous materials, due to the difficulty to assess with accuracy their particle density.

TABLE I Summary table of the main methods used for the granulometric measure of a granular sample

Methods	Principle	Interval of measurement	Main advantages (+) drawbacks (-)	Parameter determined
Sieving	Mechanical separation of particles according to their diameter through a set of sieves calibrated.	5–25000 $\mu\text{m}$	(+) $\rightarrow$ Easy and little expensive method (-) $\rightarrow$ Imprecision of the method due to the shape of the particles and their position opposite the opening of mesh	Diameter of particle, in the case of spherical particles and equivalent diameter of sieve in the other cases.
Sedimentation	Method based on the evaluation of the falling velocity of a particle in a convenient fluid. The falling velocity is directly linked to this size.	0.5–100 $\mu\text{m}$	(-) $\rightarrow$ very strict operating conditions: the choice of the fluid influences the falling velocity. (-) $\rightarrow$ The particles must be spherical, smooth and rigid in order to get acceptable results.	Stokes diameter in the case of spherical particles, or equivalent spherical diameter in the other cases.
Laser granulometry	Method based on the intensity repartition in all directions of the diffracted light by a particle. This repartition depends of the particle size.	0.04–2000 $\mu\text{m}$	(+) $\rightarrow$ Very fast obtention of granulometric repartition (few minutes) (-) $\rightarrow$ All optic models available are only applicable for spherical particle (-) $\rightarrow$ a refractive character of particles is at the origin of “ghosts” particles (-) $\rightarrow$ rather expensive method	In the case of non spherical particles a volume equivalent diameter is calculated
Resistance variation counter	Method based on the measure of the resistance variation induced by the entrance of the particles in a calibrated volume of electrolytic solution where reigns an electrical field. The volume of the particle is directly linked to the resistance variation amplitude.	1–360 $\mu\text{m}$	(+) $\rightarrow$ Very fast obtention of granulometric repartition (few minutes) (-) $\rightarrow$ risk of solubilisation or swelling of particles in the electrolytic solution. (-) $\rightarrow$ rather expensive method	A volume equivalent diameter is calculated.
Static or dynamic image analysis	Visualisation of a set of particles in 2D for a direct and individual measure of its size.		(+) $\rightarrow$ Applicable for any well-defined particle shape (sphere, cylinder, cube. . . ) (+) $\rightarrow$ This method makes also possible to evaluate others parameters like the circularity, the surface and the perimeter of each particle. (-) $\rightarrow$ The precision of the result depends on the size of the sample treated and the image-thresholding quality (-) $\rightarrow$ Time consuming (static image analysis) and expensive method.	In the case of heterogeneous particle shapes, a surface equivalent diameter is evaluated

### 2.3.2. Internal porosity

The internal porosity,  $\varepsilon_i$ , is formed by the voids inside the particle. IUPAC [16] defined for the catalysts (case of GAC) 3 types of pores according to their diameter size: the micropores (width < 2 nm), the mesopores (2 nm < width < 50 nm) and the macropores (width > 50 nm).

Generally, isotherm-adsorption studies lead to measurements of pore size, pore size distribution, and total pore volume [17]. Lowell and Shields [11], suggested another method for the determination of the total volume of micropores, which is based on a combination of two techniques: the difference between the sample volumes measured respectively by mercury porosimetry and by helium pycnometry is the volume occupied by the micropores. Indeed, with mercury porosimeters pore size determination is ranging between 300,000 nm

(under vacuum conditions) and 1.8 nm (at 400 M Pa) pore radius. So only mesopores and macropores are measured with this method.

The global internal porosity value can also be easily evaluated by a direct calculation as follows, when the solid and particle densities of material,  $\rho_s$  and  $\rho_p$ , as well as the density of pore-filling fluid,  $\rho_o$ , are known.

$$\varepsilon_i = V_{\text{pore}} / V_{\text{sample}} = (\rho_s - \rho_p) / (\rho_s - \rho_o) \quad (2)$$

When the fluid is a gas, its density,  $\rho_o$ , can be neglected with regard to that of the solid. Then, the expression becomes:

$$\varepsilon_i = 1 - (\rho_p / \rho_s) \quad (3)$$

## 2.4. Tortuosity and specific surface area

The dynamic specific surface area,  $a_{vd}$ , is defined as the ratio of the surface area actually presented by the particles to the flow to the apparent volume of solid. Except for spheres, due to a mutual overlapping of particles, its value is generally lower than that of the mostly used static specific surface area,  $a_{vs}$ , which is based on the geometrical surface area of the particles. The knowledge of  $a_{vd}$  value allows evaluating the developed bed surface area reached by the fluid flow, which corresponds to the surface area where mechanical energy dissipation as well as external liquid-solid heat and mass transfer occur.

In order to evaluate this parameter, the capillary representation of packed beds proposed by Comiti and Renaud [18] can be used. In this model, the bed is considered as a bundle of identical cylindrical tortuous pores of diameter  $d_{pore}$  and length  $L$ . If  $H$  is the bed height, the tortuosity is defined as

$$\tau = \frac{L}{H} \quad (4)$$

The diameter of the representative pore is calculated by setting that their developed surface area is identical to the fixed bed surface area really reached by the flow.

$$d_{pore} = 4\varepsilon_{ext}/[a_{vd}(1 - \varepsilon_{ext})] \quad (5)$$

The mean pore velocity is

$$U = U_0\tau/\varepsilon_{ext} \quad (6)$$

where  $U_0$  is the superficial velocity.

The knowledge of  $\tau$  and  $a_{vd}$  allows the determination of the pore Reynolds number:

$$Re_{pore} = Ud_{pore}/\nu = 4U_0\tau/[va_{vd}(1 - \varepsilon_{ext})] \quad (7)$$

which has been found to be a convenient criterion in order to characterize the flow regime transitions [19, 20].

The value of  $\tau$  and  $a_{vd}$  are determined from experimental pressure drop measurements by using the pressure drop model equation derived in [18]. This equation has been tested previously on packed beds of particles of various shapes [21–23].

$$\frac{\Delta P}{(HU_0)} = M^*U_0 + N^*, \quad \text{where } U_0 \text{ is the superficial velocity} \quad (8)$$

with

$$M^* = \left[ \left\{ 1 - \left( 1 - \frac{d_{pe}}{D} \right)^2 \right\} 0.0413 + \left( 1 - \frac{d_{pe}}{D} \right)^2 0.0968 \right] \tau^3 \rho \left( \frac{1 - \varepsilon_{ext}}{\varepsilon_{ext}^3} \right)$$

$$N^* = 2\eta\tau^2 a_{vd}^2 \left\{ 1 + \frac{4}{a_{vd}D(1 - \varepsilon_{ext})} \right\}^2 \frac{(1 - \varepsilon_{ext})^2}{\varepsilon_{ext}^3}$$

and

$$d_{pe} = 6/a_{vs}.$$

For the determination of the structural and particle parameters described above, in the case of microporous materials like granular activated carbon, some of the above cited methods proved technically unusable due to the release of air present into the microporous network. We have then developed a set of alternative methods applicable to the GAC. The elaborated operating modes, the validation procedures as well as the limits of these methods and the obtained results, are exposed in the following part. Thus, thanks to a suitable combining of various methods, all the parameters can be determined with reliability.

## 3. Experiments

### 3.1. Activated carbons

Two types of granular activated carbons commonly used in water treatment industry, were selected for this study: respectively Norit Supra Row 0.8 supplied by Norit (France), and Picactif NC 60, supplied by Pica (France). These two GAC have a vegetal origin but the manufacturing processes used to produce them induce very different aspects: opposite to Supra 0.8 which presents a well-defined cylindrical shape due to the extrusion process used to produce it, NC 60 consists in very heterogeneous granular particles. The main characteristics of each activated carbon are reported in Table II.

### 3.2. Operating procedures and results

#### 3.2.1. Image analysis

*3.2.1.1. Particle size distribution.* The granulometric characterization was obtained from static image analysis. Fig. 1 shows the image analysis bench employed in this study. It consists in a video camera CCD  $728 \times 572$  pixels, connected to a PC equipped with a grabber board and an image analysis software (Optimas 6, Bioscan).

The first step of the image analysis consists in the conversion of the colour image captured with the camera into a 8 bit grey level image on which was applied in a second step a manual threshold, then in a last step a binarization.

The granulometric characterization of the two activated carbons was obtained from the acquisition and the treatment of images of a representative sample (about 300 particles), by fitting the distribution histogram of a

TABLE II Main characteristics of activated carbons

Activated carbon	Picactif NC60	Norit Supra 0.8
Origin	Coconut	Peat charcoal
Shape	Grain	Cylinder (extruded particles)
Effective size (mm) (given by the manufacturer)	0.8–1	0.8
BET surface ( $m^2 \cdot g^{-1}$ )* (parameter evaluated for this study)	1344	1159

\*Calculated after drying in an oven at 300°C.

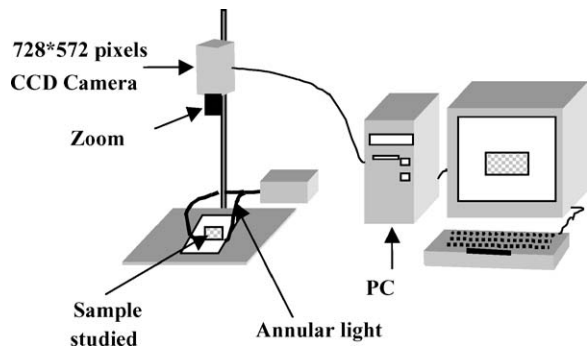


Figure 1 Image analysis bench.

characteristic dimension. This dimension is the length for the cylinders (their diameter is approximately constant) and the diameter of a disk of identical surface area for the grain. The granulometric repartition obtained in this way depends on the image-thresholding quality, therefore we have systematically made a control of the threshold. The threshold criteria lies in the check on the size of a particle in the image before binarization (i.e. 8 bit grey level image) and after binarization (i.e. white and black image). If the threshold is correctly made the size of the particle is identical in each image. To carry out this check with accuracy the size control was made on several particles located at different places of the image.

The number of examined particles required to constitute a representative sample was determined from the observation of the variation of the standard error of the measured characteristic dimension. When the value of this last one remains constant as a function of the growing number of particles examined, it can be considered that the sample size is suitable to represent the studied activated carbon.

One of the interests of this characterization lies in the possible modelling of the activated carbon size repartition by a statistical distribution law. The distribution histograms are presented in Fig. 2.

Among most common statistical laws, the gamma law proved to be a good representation of the extruded distribution. On the opposite, the size distribution of granular GAC could not be adequately modelled because of the bimodal character of the distribution.

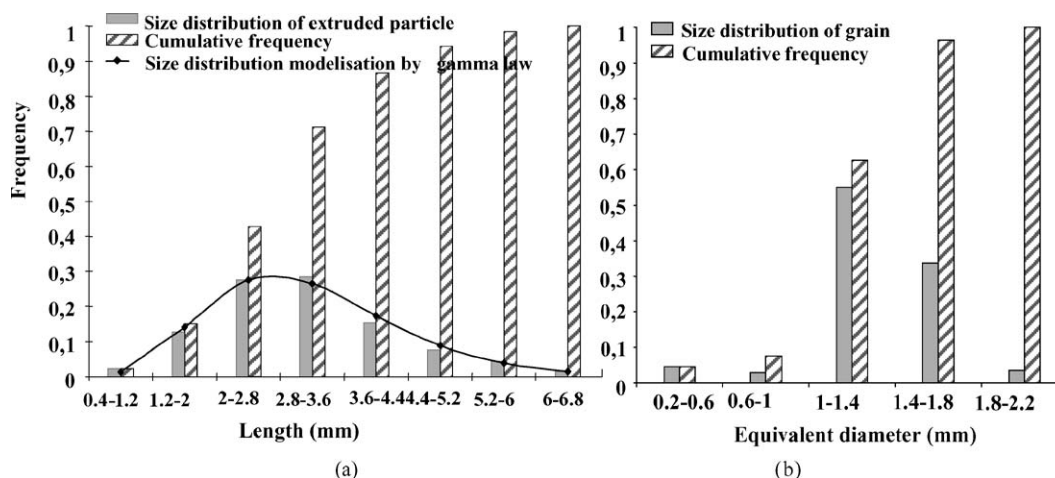


Figure 2 Extruded supra 0.8 (a) and grain NC 60 (b) repartition histograms.

TABLE III Main characteristics of the granulometric repartitions

Activated carbon particles	Average of characteristic dimension	Standard deviation
Extruded	$L_m = 3.12 \times 10^{-3}$ m	$\pm 1.4 \times 10^{-3}$ m
Grains	$D_m = 1.32 \times 10^{-3}$ m	$\pm 0.32 \times 10^{-3}$ m

The characteristics of the size distributions obtained for the two activated carbons as shown in Table III. According to the standard deviation values, the granulometric repartition of extruded GAC appears more dispersed than that of grains.

3.2.1.2. Assessment of external porosity. The experimental operating procedure includes two parts. The first step consists in consolidating an activated carbon bed in a mould ( $L_{\text{mould}} = 0.03$  m and  $D_{\text{mould}} = 0.06$  m) with a commercial epoxy liquid resin (Bueler, EPO thin), selected for its low viscosity and also because it does not shrink during its solidification. Before introducing the resin, the active carbon bed is packed down into the mould with respect to a systematic procedure developed by Ciceron [22]: successive fractions of the material corresponding to a height of one centimetre are introduced in the column, then tightly packed with a piston. Every two centimetres, a  $\pi/4$  rotation of the column is performed. The impregnation of the resin is achieved at ambient temperature under vacuum conditions in order to avoid the bubble formation due to degassing of the activated carbon. As the bed is initially tightly packed, the impregnation does not induce a variation of the bed structure.

The second step is based on the porosity estimation of different bed sections. Every 1 mm in thickness, the section of the solidified bed is captured with the camera. Taking into account the work of Montillet and Le Coq [24] which showed that end effects are generally negligible after a thickness corresponding to about two equivalent particle diameters, the first six millimetres of the bed have not been studied.

After proceeding to a manual binarization of the image of the studied section, the ratio between the solidified resin surface area located between particles and the total section surface area is determined. An

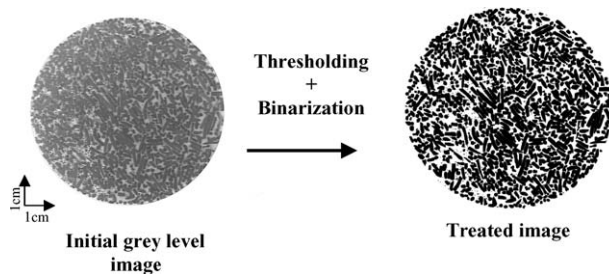


Figure 3 Bed section image before and after treatment.

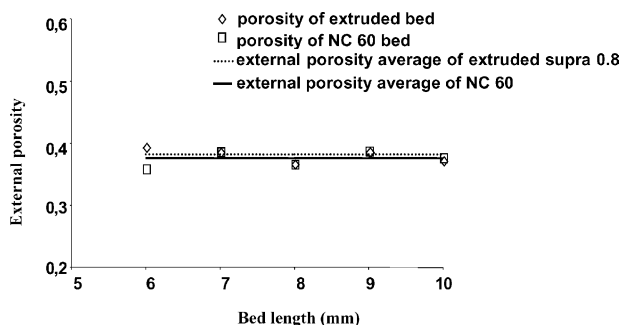


Figure 4 longitudinal porosity profiles for two activated carbon beds.

example of a raw image before and after treatment is shown in Fig. 3.

Thanks to this treatment, the evolution of the longitudinal external porosity has been determined as a function of the bed length and the mean external porosity value has been estimated.

Fig. 4 shows the longitudinal porosity variation evaluated from image analysis as a function of the bed length. The porosity profile is flat indicating that end effects do not affect the studied length. Moreover in our case, the ratio diameter  $D_{\text{mould}}/d_{\text{pe}}$  (where  $d_{\text{pe}}$  is the equivalent mean diameter of cylinder or spherical particle) is greater than 10, thereby allowing to neglect the wall effect on the mean external voidage [14].

The whole procedure applied in this study is similar to that used by Montillet and Le Coq [24] in order to determine the external porosity of two packed beds of PVC particles (rigid material). The authors notice that no modification of the shape and aspect of the particles occurs during the bed packing, nor during the resin including and hardening and nor during the bed polishing. It was confirmed by comparing the average

porosity value of bed assessed by image analysis to the value directly calculated from the particles mass introduced and the volume of the column corresponding to the bed. In our case, the thresholding sensibility on the accuracy of the porosity result was studied by modifying ( $\pm 2.5\%$ ) the suitable grey level value and was estimated to be close to 1.5% (Table IV).

The average value of the longitudinal porosity is 0.382 for the extruded supra 0.8 and 0.376 for the NC 60. This value can be considered as an estimation of the external porosity of a bed for which the end and wall effects are negligible.

### 3.2.2. Alumina pycnometry and image analysis used to determine particle density

3.2.2.1. Alumina pycnometry method. Classically, the particle density is measured using a liquid such as water. Knowing the empty pycnometer volume and measuring the adding liquid volume to fill the pycnometer in which is beforehand placed a material sample of known-mass, we assess the material solid volume. In the case of activated carbon samples, because of an incomplete air degassing at room pressure this procedure is not adequate.

In order to overcome this technical problem we have used a very fine alumina powder which granulometry has been carefully selected ( $d_p$ : 30–50  $\mu\text{m}$ ). The powder thinness is an important parameter, because it permits to minimize the interstitial volume between the alumina and solid particles. Moreover, the size of selected alumina particles prevents them to enter in the activated carbon macropores. The accuracy of this method also depends on a reproducible squeezing of alumina powder.

3.2.2.2. Image analysis operating procedure. The principle of this method consists in calculating the total volume of a known mass of sample, from 2D images. For the extruded GAC, the diameter and length of each cylinder forming the sample and then its volume can be easily determined. The particle density is then calculated as the ratio of the sample mass on the sample volume. On the other hand, due to the ill-defined shape of grains (NC 60), it is impossible to access to the real sample volume from 2D image.

TABLE IV Longitudinal porosity variation with respect the height of the bed and the thresholding grey level selected

Thresholding grey level fixed	Supra row 0.8			Thresholding grey level fixed	NC 60		
	67	69 (value selected for the manual binarization)	71		75	77 (value selected for the manual binarization)	79
Height bed observed (mm)	Porosity			Height bed observed (mm)	Porosity		
6	0.392	0.395	0.385	6	0.363	0.360	0.361
7	0.395	0.387	0.381	7	0.392	0.388	0.384
8	0.376	0.368	0.369	8	0.372	0.368	0.366
9	0.388	0.388	0.381	9	0.393	0.389	0.385
10	0.377	0.373	0.374	10	0.382	0.378	0.374
Average	0.385	0.382	0.378	Average	0.380	0.378	0.374
$D_{\text{mould}}/d_{\text{pe}}$	48			45			

3.2.2.3. *Validation of operating procedures and results.* Before applying them to the activated carbon particles, these two methods have been tested with PVC cylinders (non-porous particles) presenting the same size distribution as that of extruded supra 0.8 GAC. The obtained densities are compared to that evaluated by water pycnometry which is the classic method used to determine the density of non-porous materials.

The values of the densities as well as their experimental deviation (in square brackets) are recapped in Table V.

For each “particle-method” system tested, three measurements were carried out. The densities indicated in the table are corresponding to the average of the three obtained values. The experimental deviation (<2%) calculated between the three values, shows a good reproducibility of the operating mode used.

The difference existing between PVC cylinders density values obtained from the reference method and the others does not exceed 3.2%, permitting so to consider the results estimated with the two other suggested methods as correct. The main advantage of this double method validation lies in the possibility to determine a priori the particle density of any microporous granulate particle, with alumina pycnometry whatever its shape. Indeed, depending on the more or less shape complexity of this particle, one will choose to use either of these methods: image analysis, exclusively in the case of particles whose the shape is relatively well-defined, or the alumina pycnometry which is particularly convenient in the case of heterogeneous particle shape and which is much cheaper.

Knowing the values of the particles densities, the external porosity of corresponding activated carbon beds can be directly calculated from Equation 1. The internal porosity is evaluated from Equation 3 using the particle density and the solid density determined by helium pycnometry. The results obtained were presented in Table VI.

The external porosity values obtained by direct calculation are in good agreement with these obtained from image analysis (Section 3.2.1) corroborating then the validity of the particle density values determined previously by alumina pycnometry.

The internal porosity values existing in the literature concerning activated carbon grains obtained by a physical activation extend, according to the authors, from 0.49 [25] to 0.78 [26]. This disparity finds its origin in different factors [25, 26] such as the raw material,

TABLE V Particle density of PVC cylinders (validation step), extruded and granulate activated carbon

Particles types	Methods		
	Water pycnometry	Alumina pycnometry	Image analysis
PVC cylinders (kg·m <sup>-3</sup> )	1150 (±0.5%)	1113 (±0.9%)	1147 (±1.09%)
Supra 0.8 (kg·m <sup>-3</sup> )	Inadequate method	642 (±1.4%)	635 (±0.3%)
NC 60 (kg·m <sup>-3</sup> )	Inadequate method	880 (±1.5%)	Inadequate method

TABLE VI Internal and external porosities evaluated for Supra 0.8 and NC60 beds

	Supra 0.8	NC 60
<sup>1</sup> Solid density (kg·m <sup>-3</sup> )	1950	2020
Particle density (kg·m <sup>-3</sup> )	642	880
$\epsilon_{\text{ext}}$ (Equation 1)	0.37	0.40
$\epsilon_{\text{ext}}$ (image analysis)	0.38	0.38
$\epsilon_i$ (Equation 3)	0.67	0.56

<sup>1</sup>The solid density was determined by helium pycnometry.

the parameters of activation step, and the methods employed to determine the pore volume of the granule.

### 3.2.3. Permeametry method used to determine the dynamic specific surface area and the hydraulic tortuosity

Fig. 5 shows the cylindrical column used for the pressure drop measurements ( $D = 0.06$  m and  $H = 0.3$  m) where homogeneous beds of dry activated carbon particles were packed with respect to a systematic procedure developed by Ciceron [22]: successive fractions of the material corresponding to a height of one centimetre are introduced in the column, then tightly packed. Every 2 centimetres, a  $\pi/4$  rotation of the column of is performed.

The flowing liquid was demineralised water maintained at  $23^\circ\text{C} \pm 0.3^\circ\text{C}$  and the pressure drop through the bed height of 0.2 m was measured using a U-tube manometer. The results obtained are plotted as  $\frac{\Delta P}{HU_0}$  as a function of  $U_0$ .

The obtained results are presented in Figs 6 and 7. For each type of GAC the graph includes the pressure drop measurements carried within two distinct beds.

For supra 0.8 fixed beds (in S.I. Units):

$$\Delta P/HU_0 = 1.59 \times 10^7 U_0 + 6.97 \times 10^5 \quad (\delta = 1\%) \quad (9)$$

with

$$\delta = 100 \times \frac{1}{N} \sum_1^N \left| \frac{\frac{\Delta P}{HU_0}(\text{measured}) - \frac{\Delta P}{HU_0}(\text{correlated})}{\frac{\Delta P}{HU_0}(\text{measured})} \right| \quad (10)$$

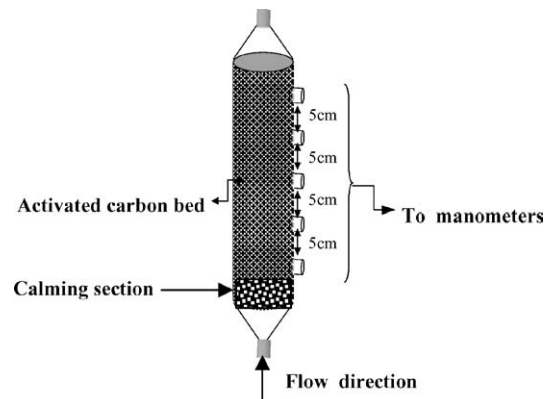


Figure 5 Test column for the pressure drop measurements.

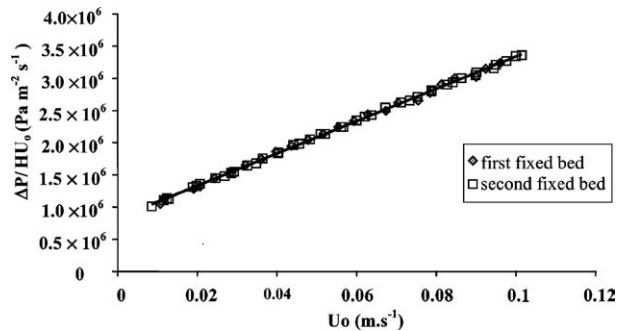


Figure 6 Variation in  $\Delta P/HU_0$  with  $U_0$  for the supra 0.8 fixed beds.

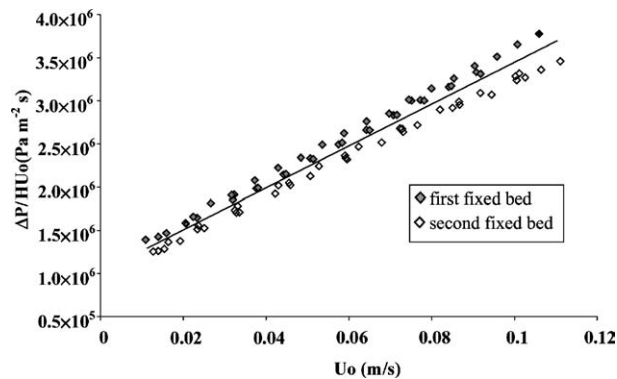


Figure 7  $\Delta P/HU_0$  versus  $U_0$  for the NC 60 fixed beds.

And for NC 60 beds in S.I. Units:

$$\Delta P/HU_0 = 2.35 \times 10^7 U_0 + 1.07 \times 10^6 \quad (\delta = 5\%) \quad (11)$$

The dispersion of data corresponding to the NC 60 beds is bigger than that of supra 0.8. It can be explained by a worse packing reproducibility of NC 60 beds due to the heterogeneous shape of this GAC.

TABLE VII Structural parameters

Type of particle	$\varepsilon_{\text{ext}}$	$\tau$	$a_{\text{vs}}$ ( $\text{m}^{-1}$ )	$a_{\text{vd}}$ from pressure drops ( $\text{m}^{-1}$ )	$a_{\text{vd}}/a_{\text{vs}}$	$a_v$ from BET method ( $\text{m}^{-1}$ )
Supra 0.8	0.37	1.41	5158	4871	0.944	$7.4 \cdot 10^8$
NC60	0.4	1.63	—	6219		
PVC cylinders	0.35	1.62	4513	4100	0.905	$11.7 \cdot 10^8$

3.2.3.1. *Results and discussion.* The external porosity value being known by using alumina pycnometry or image analysis, the values of  $a_{\text{vd}}$  and  $\tau$  are estimated by experiment-model identification using Equation 8.

The obtained results with the two types of GAC as well as with non-microporous PVC cylinders are given in Table VII.

For the cylindrical porous and non-porous particles the ratio between the  $a_{\text{vd}}$  and  $a_{\text{vs}}$  value obtained from image analysis shows a small degree of mutual overlapping of the particles in the bed. The slightly higher value of this ratio obtained for GAC extruded particles can be explained by the microparticles roughness effect.

For the NC 60, owing to the three-dimensional shape of the particles, image analysis could not be used to obtain an order of magnitude of the specific surface area,  $a_{\text{vs}}$ , only the permeametry method is available in this case. Finally one can notice the great difference between  $a_{\text{vs}}$  or  $a_{\text{vd}}$  and the specific surface area determined by BET which takes into account the external surface area of the particles as well as the surface area on the internal pores. Indeed, this result is consistent because the internal surface area of the micropores where adsorption occurs is much more important than the external surface area of the particles.

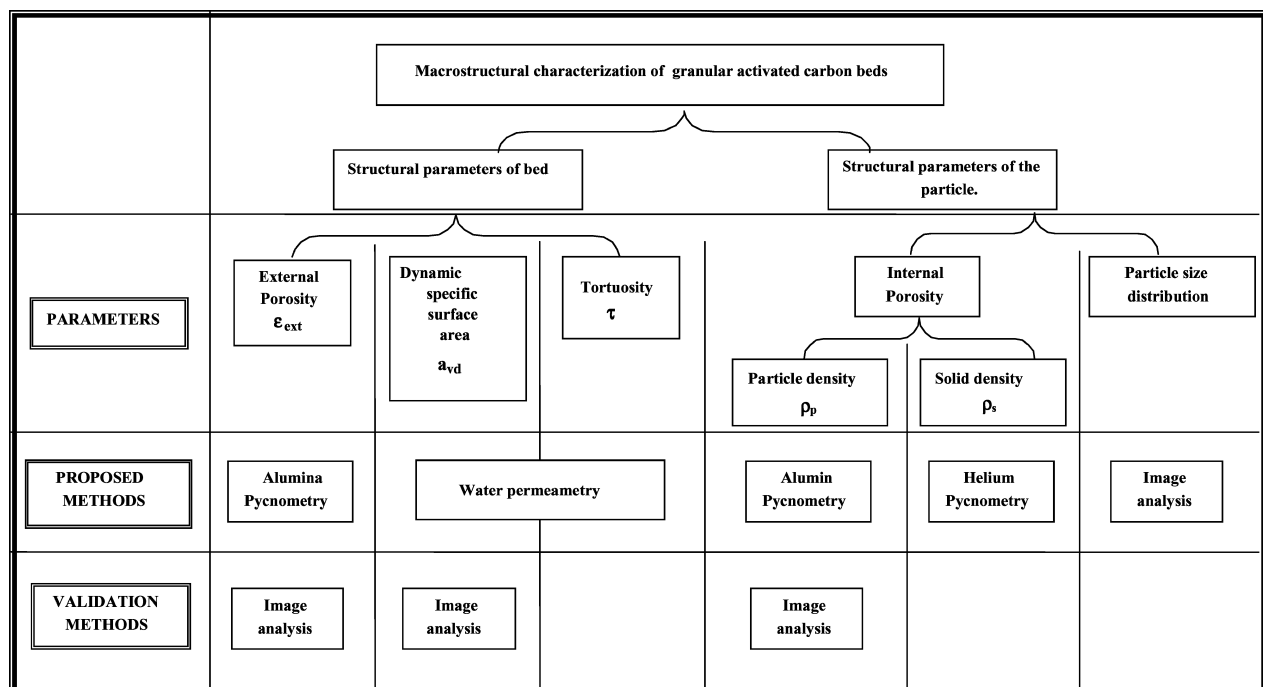


Figure 8 Global diagram of the different steps in the characterization of studied activated carbons.

#### 4. Conclusion

In this paper a set of simple and accurate methods is proposed to obtain the bed and particle structural parameters of microporous particles. It has been used in order to characterize two different types of GAC used in packed beds for water depollution. The obtained results have been checked by using validation methods based on image analysis. A summary diagram recapping the experimental approach is proposed in Fig. 8.

#### References

1. C. SOLISIO, A. LODI and M. DEL BORGUI, *Waste Management* **21** (2000) 33.
2. K. S. KNAEBEL, a "How" Guide for Adsorber Design, Private Report (2000).
3. J. L. SOTELO, G. OVEJERO, J. A. DELGADO and I. MARTINEZ, *Chem. Engng. J.* **87** (2002) 111.
4. N. KANNAN and M.M. SUNDARAM, *Dyes and Pigments* **51** (2001) 25.
5. J. ROUQUEROL, D. AVNIR, C. W. FAIBRIDGE, D. H. EVERETT, J. H. HAYNES, N. PERNOCON, J. D. F. RAMSAY, K. S. W. SING and K. K. UNGER, *Pure & Appl. Chem.* **66** (1994) 1739.
6. M. KRUCK, M. JARONIEC and J. CHOMA, *Carbon* **36** (1998) 1447.
7. D. PAN, M. JARONIEC and J. KLINIC, *ibid.* **34** (1996) 1109.
8. M. JARONIEC, K. P. GADKAREE and J. CHOMA, *Colloids Surfaces A: Physicochem. Eng. Aspects* **118** (1996) 203.
9. A. SCHÜLE, W. RASEMANN and C. PREUSSE, *Part. Part. Syst. Charact.* **14** (1997) 21.
10. J. P. MELCION, *INRA Prod. Anim.* **13** (2000) 81.
11. S. LOWELL and J. E. SHIELDS, "Powder Surface Area and Porosity" (Chapman & Hall, London, 1984).
12. R. ENGLAND and D. J. GUNN, *Trans. Instn Chem. Engrs.* **48** (1970) 265.
13. A. G. DIXON, *Can. J. Chem. Engng.* **66** (1988) 705.
14. E. A. FOUHENY and S. ROSHANI, *Chem. Engng. Sci.* **46** (1991) 2363.
15. R. P. ZOU and A. B. YU, *ibid.* **51** (1996) 1177.
16. IUPAC and D. H. EVERETT, *Pure & Appl. Chem.* **31** (1972) 579.
17. R. S. JUANG, F. C. WU and R. L. TSENG, *J. Chem. Engng. Data* **41** (1996) 487.
18. J. COMITI and M. RENAUD, *Chem. Engng. Sci.* **44** (1989) 1539.
19. D. SEGUIN, A. MONTILLET and J. COMITI, *ibid.* **53** (1998) 3751.
20. D. SEGUIN, A. MONTILLET, J. COMITI and F. HUET, *ibid.* **53** (1998) 3897.
21. N. E. SABIRI and J. COMITI, *Can. J. Chem. Engng.* **75** (1997) 1030.
22. D. BRUNJAIL and J. COMITI, *Chem. Engng. J.* **45** (1990) 23.
23. D. CICERON, J. COMITI and R. P. CHHABRA, *Chem. Eng. Comm.* **189** (2002) 1403.
24. A. MONTILLET and L. LE COQ, *Powder Technol.* **121** (2001) 138.
25. G. DRAZER, R. CHERTCOFF, L. BRUNO, M. ROSEN and J. P. HULIN, *Chem. Engng. Sci.* **54** (1999) 4137.
26. D. MOHAN, V. K. GUPTA, S. K. SRIVASTAVA and S. CHANDER, *Colloids and Surface A: Physicochem. Eng. Aspects* **177** (2001) 169.

Received 2 December 2002  
and accepted 14 October 2004